Article

Cell Reports

HIF-1-Mediated Suppression of Acyl-CoA Dehydrogenases and Fatty Acid Oxidation Is Critical for Cancer Progression

Graphical Abstract

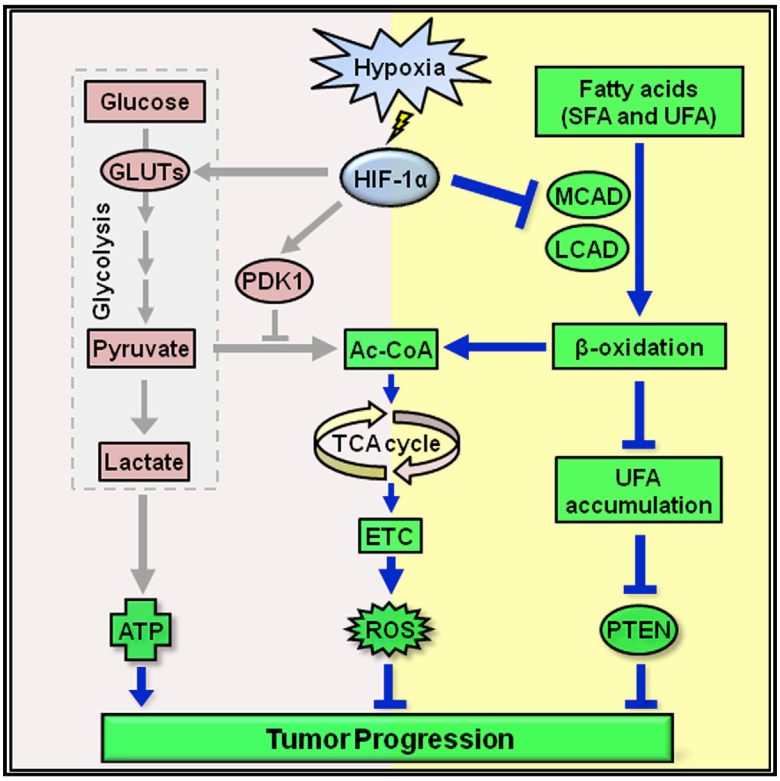

Highlights

HIF-1 suppresses FAO in cancer cells by inhibiting MCAD and LCAD expression

HIF-1-mediated FAO suppression promotes cancer proliferation in part by reducing ROS

Suppression of LCAD, but not MCAD, blunted PTEN expression and enhanced tumor growth

Decreased LCAD expression in human HCC predicts patient mortality

Authors

De Huang, Tingting Li, ..., Ping Gao, Huafeng Zhang

Correspondence

hzhang22@ustc.edu.cn

In Brief

Hypoxia, via activation of HIF-1, is known to inhibit fatty acid oxidation (FAO) as part of the metabolic reprogramming of cancer cells, but the mechanisms linking FAO and cancer progression are unclear. Huang et al. now report that HIF-1 inhibition of two FAO enzymes, the acyl-CoA dehydrogenases MCAD and LCAD, promotes cancer progression via effects on ROS and glycolysis and that LCAD loss further promotes cancer by regulating the PTEN pathway, highlighting the significance of FAO inhibition in cancer.

Huang et al., 2014, Cell Reports 8, 1930–1942
September 25, 2014 ©2014 The Authors
http://dx.doi.org/10.1016/j.celrep.2014.08.028

OPEN ACCESS
CellPress

Cell Reports
Article

HIF-1-Mediated Suppression of Acyl-CoA Dehydrogenases and Fatty Acid Oxidation Is Critical for Cancer Progression

De Huang,[1] Tingting Li,[1] Xinghua Li,[2] Long Zhang,[1] Linchong Sun,[1] Xiaoping He,[1] Xiuying Zhong,[1] Dongya Jia,[1] Libing Song,[2] Gregg L. Semenza,[3] Ping Gao,[1] and Huafeng Zhang[1,*]

[1]Institute for Cancer Research and CAS Key Laboratory of Innate Immunity and Chronic Disease, Innovation Center for Cell Biology, School of Life Science, University of Science and Technology of China, Hefei 230027, China

[2]State Key Laboratory of Oncology in Southern China and Departments of Experimental Research, Sun Yat-sen University Cancer Center, Guangzhou 510060, China

[3]Johns Hopkins University School of Medicine, Baltimore, MD 21205, USA

*Correspondence: hzhang22@ustc.edu.cn

http://dx.doi.org/10.1016/j.celrep.2014.08.028

SUMMARY

Hypoxia-inducible factor 1 (HIF-1) mediates a metabolic switch that blocks the conversion of pyruvate to acetyl-CoA in cancer cells. Here, we report that HIF-1α also inhibits fatty acid β-oxidation (FAO), another major source of acetyl-CoA. We identified a PGC-1β-mediated pathway by which HIF-1 inhibits the medium- and long-chain acyl-CoA dehydrogenases (MCAD and LCAD), resulting in decreased reactive oxygen species levels and enhanced proliferation. Surprisingly, we further uncovered that blocking LCAD, but not MCAD, blunts PTEN expression and dramatically affects tumor growth in vivo. Analysis of 158 liver cancer samples showed that decreased LCAD expression predicts patient mortality. Altogether, we have identified a previously unappreciated mechanism by which HIF-1 suppresses FAO to facilitate cancer progression.

INTRODUCTION

The reprogramming of cellular energy metabolism is one of the recognized ''emerging hallmarks'' of human cancer (Hanahan and Weinberg, 2011). Warburg first observed that compared to normal cells, cancer cells have increased conversion of glucose to lactate (Vander Heiden et al., 2009). Because metabolism is a fundamental activity that determines cellular fate, tremendous effort has been made in the past 2 decades to understand the molecular mechanisms underlying its reprogramming in cancer cells (DeBerardinis and Thompson, 2012). For instance, hypoxia-inducible factor 1 (HIF-1) mediates a metabolic switch that shunts glucose metabolites away from the mitochondria (Kim et al., 2006). HIF-1 regulates the expression of pyruvate dehydrogenase kinase 1, which inactivates pyruvate dehydrogenase, the enzyme that catalyzes the conversion of pyruvate to acetyl-CoA for entry into the tricarboxylic acid (TCA) cycle. Mitochondrial respiration under prolonged hypoxic conditions results in increased generation of reactive oxygen species (ROS) and cell death (Kim et al., 2006). Hence, metabolic reprogramming to limit acetyl-CoA generation and TCA cycle activity is an adaptive strategy for cells in the hypoxic microenvironment that is characteristic of advanced cancers. However, whereas acetyl-CoA is also generated by fatty acid β-oxidation (FAO), it remains poorly understood what adaptations may occur to FAO during cancer progression.

HIF-1 was reported to regulate the expression of fatty acid synthase (FASN) and lipin 1 (LPIN1) (Furuta et al., 2008; Mylonis et al., 2012), which facilitate fatty acid synthesis (FAS) and lipid storage, which are adaptive metabolic responses to hypoxia (Menendez and Lupu, 2007). Hypoxia was also reported to diminish FAO in cultured cardiac myocytes (Huss et al., 2001) and in cardiac hypertrophy models in a HIF-1-dependent manner (Krishnan et al., 2009). However, contradictory evidence exists regarding the consequences of fatty acid catabolism, or FAO, for cancer progression (Deberardinis et al., 2006; Zaugg et al., 2011). Obviously, the beneficial role of FAO for cancer growth may be context dependent, or cancer cell type specific, and more extensive investigations are warranted to understand the effect of cancer metabolic reprogramming on FAO.

In this study, we screened human hepatocellular carcinoma (HCC) cells for genes encoding lipid metabolic enzymes that are regulated by hypoxia through HIF-1. We report here a previously unappreciated mechanism by which HIF-1 suppresses the medium-chain (MCAD) and long-chain (LCAD) acyl-CoA dehydrogenases and FAO to facilitate cancer progression by cross-talk between metabolic and signal transduction pathways.

RESULTS

Hypoxia Suppresses FAO in Cancer Cells in a HIF-1-Dependent Manner

We first investigated if hypoxic stress regulates lipid metabolism in human HCC cells. We cultured Hep3B, SK-Hep-1, and HepG2 cells under nonhypoxic (20% O_2) or hypoxic (1% O_2) conditions

for 48 hr. Nile red staining and triglyceride (TG) measurement in cell lysates revealed that hypoxic stress led to significant lipid accumulation in all three cancer cell lines (Figures 1A and 1B). Because HIF-1 plays a major role in hypoxia-induced reprogramming of glucose metabolism in cancer cells, we next explored whether HIFs are involved in the altered lipid metabolism induced by hypoxic stress. We established Hep3B cells stably expressing a nontargeting control (NTC) short hairpin RNA (shRNA) or shRNA targeting HIF-1α, HIF-2α, or both (double knockdown, DKD) (Figure 1C). Downregulation of HIF-1α or HIF-2α or both attenuated hypoxia-induced lipid accumulation (Figures 1D and 1E), indicating that both HIF-1α and HIF-2α regulate lipid metabolism in Hep3B cells.

To address the mechanisms underlying hypoxia-induced lipid accumulation in cancer cells, we utilized a pathway-focused PCR array of genes encoding lipid metabolic enzymes and cDNA prepared from Hep3B cells that were cultured under nonhypoxic or hypoxic conditions for 36 hr. Based on the PCR array results, we designed primers and performed reverse transcription and quantitative real-time PCR to confirm the expression of genes that were hypoxia responsive in the array analysis. It is intriguing that several major genes responsible for lipid synthesis and lipid catabolism, or β-oxidation, were regulated by hypoxia (Figure 1F). As reported (Furuta et al., 2008; Mylonis et al., 2012), we observed hypoxia-induced expression of several genes regulating lipid synthesis, including *FASN* and *LPIN1*. Interestingly, several lipid catabolism genes, especially *MCAD* and *LCAD*, were downregulated under hypoxic conditions in Hep3B cells (Figure 1F), as well as in HepG2 and PC3 prostate cancer cells (Figures S1A and S1B). Because MCAD and LCAD are key enzymes catabolizing the first step of FAO in mitochondria, our observation that hypoxic stress dramatically inhibits MCAD and LCAD expression suggests that FAO is suppressed in hypoxic cancer cells, which might contribute to hypoxia-induced lipid accumulation.

To test our hypothesis, we measured the FAO rate using [1-^{14}C]-palmitic acid or [1-^{14}C]-oleic acid in Hep3B cells. The conversion rate of palmitic acid or oleic acid into either acid-soluble metabolites (ASM) or CO_2 was measured under nonhypoxic and hypoxic conditions, or in the presence of etomoxir, an FAO inhibitor. As expected, etomoxir decreased levels of ASM and CO_2 produced from [1-^{14}C]-palmitic acid in Hep3B cells (Figure 1G). Interestingly, levels of ASM and CO_2 produced from either [1-^{14}C]-palmitic acid (Figure 1G) or [1-^{14}C]-oleic acid (Figure 1H) are significantly inhibited in hypoxic Hep3B cells. Similar results were observed in SK-Hep-1 (Figure S1C) and PC3 cells (Figure S1D), suggesting that hypoxic stress inhibits FAO in cancer cells. Further studies using Hep3B cells that stably expressed shRNAs targeting HIFs revealed that, in HIF-1α knockdown or DKD cells, but not HIF-2α knockdown cells, hypoxia-induced inhibition of [1-^{14}C]-palmitic acid or [1-^{14}C]-oleic acid oxidation was attenuated (Figures 1I and 1J), indicating that HIF-1α, but not HIF-2α, is required for inhibition of FAO in hypoxic Hep3B cells.

HIF-1α Suppresses FAO by Inhibiting the Expression of MCAD and LCAD

We next asked whether MCAD and LCAD are key enzymes responsible for HIF-1-mediated regulation of FAO and lipid reprogramming in cancer cells. MCAD and LCAD belong to the acyl-CoA dehydrogenase family that also includes short-chain (SCAD) and very-long-chain (VLCAD) acyl-CoA dehydrogenases (Kunau et al., 1995). Among the family members, MCAD and LCAD protein levels were significantly decreased under hypoxia in all of the cell lines analyzed, including Hep3B, SK-Hep-1, and HepG2 HCC cells, as well as PC3 prostate cancer and MCF-7 breast cancer cells (Figures 2A and S2A). Of note, hypoxia did have some effects on the expression of CPT1A or CPT1C in cell lines such as MCF-7, as previously reported (Zaugg et al., 2011). However, we did not observe those effects in Hep3B cells (Figures 2A and S2A). We thus focused on MCAD and LCAD for further study.

Treatment of Hep3B cells with $CoCl_2$ or desferrioxamine, which are chemical inducers of HIF activity, also inhibited the expression of MCAD and LCAD in a time-dependent manner (Figure S2B). Knockdown of HIF-1α, but not HIF-2α, expression attenuated the inhibitory effect of hypoxia on the expression of MCAD and LCAD mRNA (Figure 2B) and protein (Figure 2C) in Hep3B cells. Knockdown of HIF-1α expression in SK-Hep-1 or PC3 cells had the same effect (Figures S2C and S2D). Moreover, hypoxia failed to decrease MCAD and LCAD levels in HIF-1α knockout mouse embryonic fibroblasts (KO-MEF) (Figure S2E), which provided further evidence that HIF-1α is critical for hypoxia-induced downregulation of MCAD and LCAD expression.

Next, we investigated the mechanism by which HIF-1α downregulates the expression of MCAD and LCAD, which catalyzes the first step of FAO in mitochondria. Interestingly, we found that hypoxia significantly decreased the expression of PGC-1β, a transcription factor that plays critical roles in regulating mitochondrial function, in Hep3B cells as well as in HepG2 and PC3 cells (Figures 2D and S2F). When PGC-1β expression was knocked down, MCAD and LCAD mRNA and protein expression were significantly suppressed in Hep3B (Figures 2E and 2F) and PC3 cells (Figures S2G and S2H), suggesting that PGC-1β is directly involved in transcriptional regulation of MCAD and LCAD, which is consistent with previous reports (Lin et al., 2005; Espinoza et al., 2010). We have documented previously that both HIF-1α and HIF-2α inhibit PGC-1β through c-Myc suppression in VHL-null RCC4 renal carcinoma cells (Zhang et al., 2007). Here, we found that hypoxic stress repressed c-Myc and PGC-1β in Hep3B and PC3 cells (Figure S2I). Moreover, western blot assays of Hep3B cells expressing HIF shRNAs revealed that HIF-1α, but not HIF-2α, repressed c-Myc and PGC-1β expression under hypoxia (Figure 2C), which is consistent with our finding that HIF-1α, but not HIF-2α, downregulated MCAD and LCAD expression under hypoxia. Moreover, downregulation of c-Myc by shRNA blocked the expression of PGC-1β, MCAD, and LCAD, whereas forced expression of c-Myc enhanced their expression in Hep3B cells (Figure S2J). Decreased mRNA and protein levels of PGC-1β, MCAD, and LCAD were also observed in c-Myc-depleted tetracycline-inducible P493 cells (Figures S2K and S2L), further confirming that c-Myc regulates expression of PGC-1β, which, in turn, regulates the expression of MCAD and LCAD. Forced expression of c-Myc counteracted the hypoxia-induced decrease of PGC-1β, MCAD, and LCAD protein levels (Figure 2G), suggesting that

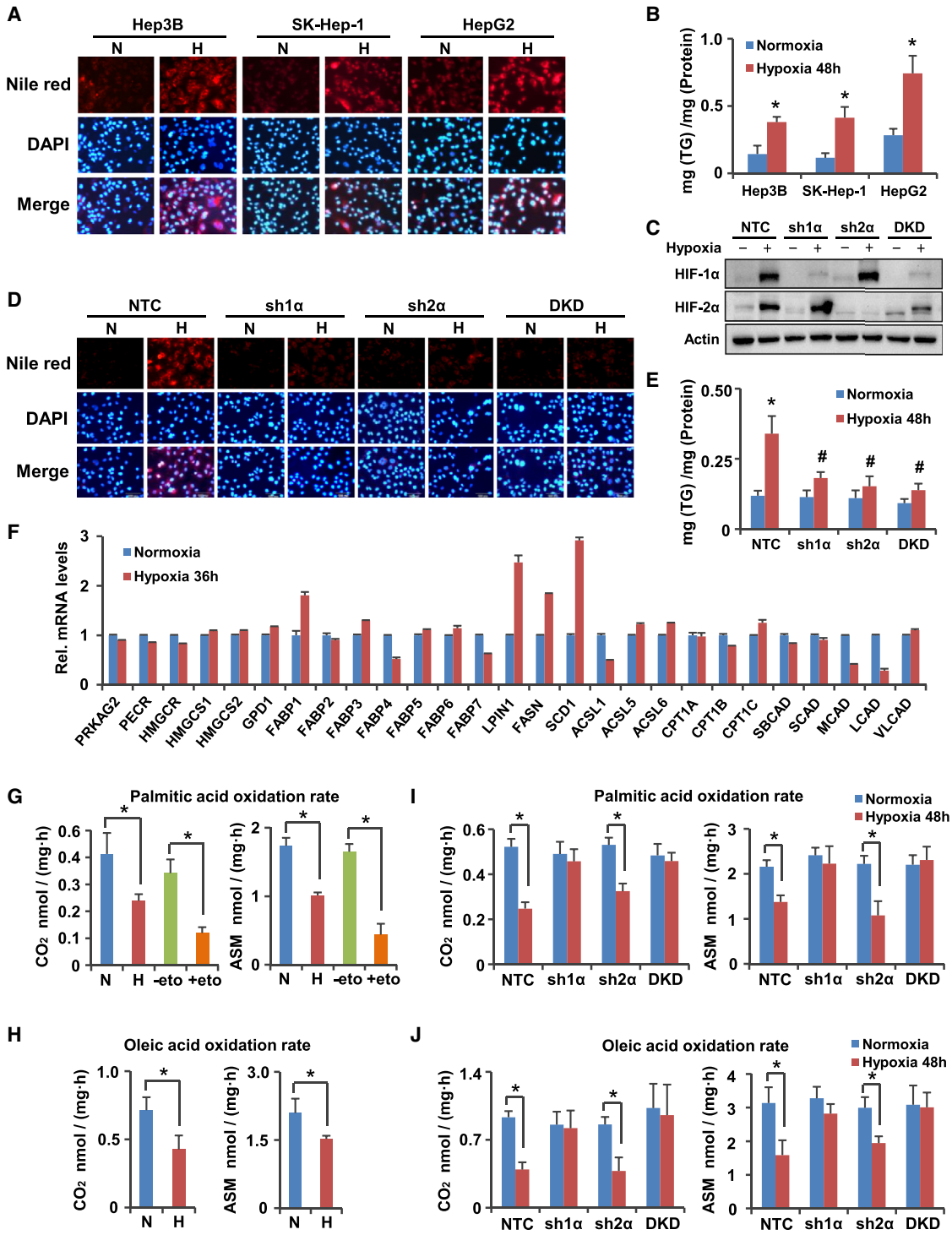

Figure 1. Hypoxia Suppresses Fatty Acid Oxidation in Cancer Cells in a HIF-1-Dependent Manner

(A) Hep3B, SK-Hep-1 and HepG2 cells were incubated under normoxia or hypoxia for 48 hr, followed by staining with Nile Red and DAPI.

(B) Hep3B, SK-Hep-1, and HepG2 cells were cultured under normoxia or hypoxia for 48 hr. Cellular TG content was measured using the triglyceride detection kit. The values were normalized to cellular protein.

(C) Western blot analysis of HIF-1α and HIF-2α in Hep3B cells stably expressing nontargeting control shRNA (NTC), HIF-1α shRNA (sh1α), HIF-2α shRNA (sh2α), or HIF-1α shRNA plus HIF-2α shRNA (double knockdown, DKD) under normoxia or hypoxia for 4 hr.

(D and E) Hep3B cells stably expressing NTC, sh1α, sh2α, or DKD were treated under normoxia or hypoxia for 48 hr followed by Nile Red and DAPI staining (D) or cellular TG measurement (E).

(legend continued on next page)

HIF-1α-mediated suppression of the c-Myc → PGC-1β axis is involved in hypoxic regulation of MCAD and LCAD expression.

To investigate whether MCAD and LCAD are involved in HIF-1α-regulated FAO suppression under hypoxia, Hep3B cells were stably transfected with control pSIN-GFP vector or vector encoding MCAD or LCAD or both (Figure 2J). FAO analysis using [1-^{14}C]-palmitic acid, [1-^{14}C]-stearic acid, [1-^{14}C]-oleic acid, or [1-^{14}C]-linoleic acid revealed that forced expression of MCAD recovered hypoxia-inhibited ASM production from [1-^{14}C]-palmitic acid and [1-^{14}C]-stearic acid (Figures 2H and S2M), whereas LCAD overexpression recovered hypoxia-inhibited ASM production from [1-^{14}C]-oleic acid and [1-^{14}C]-linoleic acid (Figures 2I and S2N), providing evidence that MCAD and LCAD are critical targets for hypoxia-induced repression of FAO. Palmitic acid and stearic acid are saturated fatty acids, whereas oleic acid and linoleic acid are unsaturated fatty acids. Our results suggested that MCAD and LCAD may function in saturated and unsaturated FAO, respectively. To confirm this hypothesis, we generated Hep3B cells stably expressing control shRNA, or shRNAs targeting MCAD, LCAD, or both (Figure 2M). FAO analysis showed that MCAD knockdown primarily repressed the palmitic acid and stearic acid oxidation rates (Figures 2K and S2O), whereas LCAD knockdown primarily inhibited the oleic acid and linoleic acid oxidation rates (Figures 2L and S2P), confirming our observation that MCAD and LCAD mostly mediate saturated and unsaturated fatty acids oxidation, respectively. It should be noted that LCAD knockdown appears to slightly reduce saturated fatty acids oxidation, whereas MCAD knockdown also reduces marginally unsaturated fatty acids oxidation, but the effects are obviously not enough to attain significance. Nile red staining and TG content measurements showed that inhibition of MCAD or LCAD led to lipid accumulation (Figures S2Q and S2R). Forced expression of both MCAD and LCAD diminished the hypoxia-induced accumulation of lipid and TGs in Hep3B cells (Figures S2S and S2T), suggesting that both MCAD- and LCAD-dependent FAO contributed to the hypoxia-induced lipid accumulation. It should be noted that forced expression of either MCAD or LCAD alone only marginally reduced hypoxia-induced lipid accumulation and TG content elevation (Figures S2S and S2T), suggesting that inhibition of both saturated and unsaturated FAO mediated by MCAD and LCAD, respectively, is involved in elevated lipid accumulation under hypoxic stress.

MCAD and LCAD Regulate Cell Proliferation in Part by Altering ROS Levels

Because we have confirmed that MCAD and LCAD regulate lipid metabolism in cancer cells, we next investigated the effect of MCAD or LCAD on cancer cell proliferation. Our results revealed that MCAD- or LCAD-specific shRNA-stimulated cancer cell growth compared to the nontargeting control shRNA (Figures 3A–3C). Moreover, cells expressing LCAD shRNA appeared to have a greater growth advantage than those expressing MCAD shRNA (Figures 3B and 3C). Similar results were observed in Hep3B cells expressing another shRNA for MCAD or LCAD (shMCAD-2 or shLCAD-2) (Figure S3A) and SK-Hep-1 cells expressing MCAD or LCAD shRNA (Figures S3B and S3C), suggesting that MCAD and especially LCAD possess tumor-suppressive effects. However, forced expression of MCAD, LCAD, or both in Hep3B cells showed no obvious effect on cell growth under nonhypoxic conditions (Figure 3D), whereas, under hypoxic conditions, forced expression of LCAD significantly inhibited cell growth as compared to GFP-expressing control Hep3B cells (Figures 3E and 3F). Although overexpression of MCAD did not inhibit cell growth (Figure S3D), simultaneous expression of MCAD and LCAD manifested more potent inhibition of cell growth than LCAD alone under hypoxia (Figures 3E and 3F).

In mitochondria, FAO generates acetyl-CoA, which enters the TCA cycle to generate NADH, which donates electrons to the electron transport chain (ETC) that eventually are used by complex IV to reduce O_2 to H_2O. To investigate if MCAD and LCAD affect cell proliferation by regulating cellular ROS levels, ROS scavengers N-acetyl-cysteine (NAC, 5 mM) or glutathione (GSH, 5 mM) were added to the culture media of Hep3B cells. NAC or GSH eliminated the mild stimulating effect of MCAD shRNA on cell proliferation (Figures 3B and 3C). Interestingly, although NAC or GSH treatment partially reduced the difference in proliferation between cells expressing shLCAD and those expressing NTC shRNA, cells expressing shLCAD still showed a growth advantage, even in the presence of NAC or GSH (Figures 3B and 3C). Similar results were observed in SK-Hep-1 cells (Figure S3C). Under hypoxic conditions, NAC or GSH also partially rescued the growth inhibition caused by forced expression of LCAD (Figures 3E and 3F). Cellular ROS measurement by dichlorofluorescein (DCF) staining and flow cytometry revealed reduced ROS levels in MCAD or LCAD knockdown cells as compared to the control group in Hep3B cells (Figures 3G, 3H, and S3E) as well as in SK-Hep-1 cells (Figures S3F and S3G). Overexpression of MCAD, LCAD, or both did not lead to significant changes in ROS levels under nonhypoxic conditions (Figure 3I). However, under hypoxia, ROS levels were significantly increased in MCAD- or LCAD-overexpressing cells, as well as in cells with coexpression of MCAD and LCAD (Figure 3J). Treatment with etomoxir decreased ROS levels in Hep3B cells (Figure S3E). Taken together, these data indicate that inhibition of MCAD and LCAD diminished cellular ROS levels by modulating FAO and mitochondrial respiration. MCAD and LCAD modulate

(F) Quantitative real-time PCR analyzed the mRNA expression of different enzymes involved in fatty acid metabolism in Hep3B cells treated under normoxia or hypoxia for 36 hr.

(G and H) Hep3B cells were cultured under normoxia or hypoxia for 48 hr in the presence of [1-^{14}C]-palmitic acid (G) or [1-^{14}C]-oleic acid (H). Oxidation rates were measured using the conversion rate of radiolabeled palmitic acid or oleic acid into either ASM or CO_2. Etomoxir (eto) (100 μM) was used as a positive control (G).

(I and J) Oxidation rates of [1-^{14}C]-palmitic acid (I) or [1-^{14}C]-oleic acid (J) were measured in Hep3B cells stably expressing NTC, sh1α, sh2α, or DKD treated under normoxia or hypoxia for 48 hr, using the produced radioactive ASM and CO_2.

β-actin serves as loading control in the western blot. Data were presented as mean (±SD). *$p < 0.05$ as compared to corresponding control group; #$p < 0.05$ as compared to hypoxia-treated NTC group. See also Figure S1.

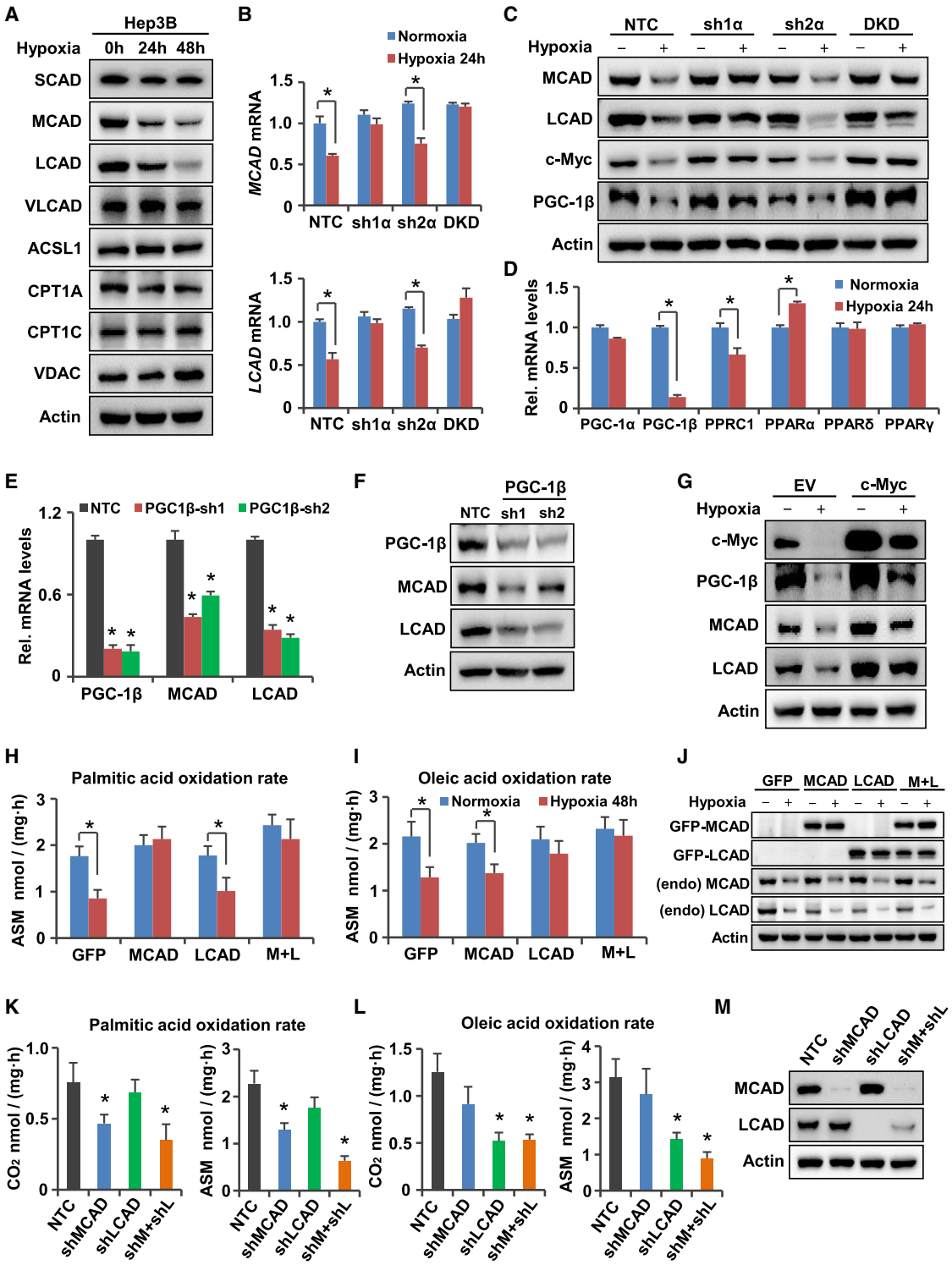

Figure 2. HIF-1α Suppresses Fatty Acid Oxidation by Inhibiting the Expression of MCAD and LCAD

(A) Western blot analysis of the proteins associated with FAO in Hep3B cells cultured under normoxia or hypoxia for 24 and 48 hr.

(B) Quantitative real-time PCR analysis of *MCAD* and *LCAD* mRNA expression in Hep3B cells stably expressing NTC, sh1α, sh2α, or DKD cultured under normoxia or hypoxia for 24 hr.

(C) Hep3B cells stably expressing NTC, sh1α, sh2α, or DKD were cultured under normoxia or hypoxia for 48 hr, followed by western blot analyzing protein expression of MCAD, LCAD, c-Myc, and PGC-1β.

(legend continued on next page)

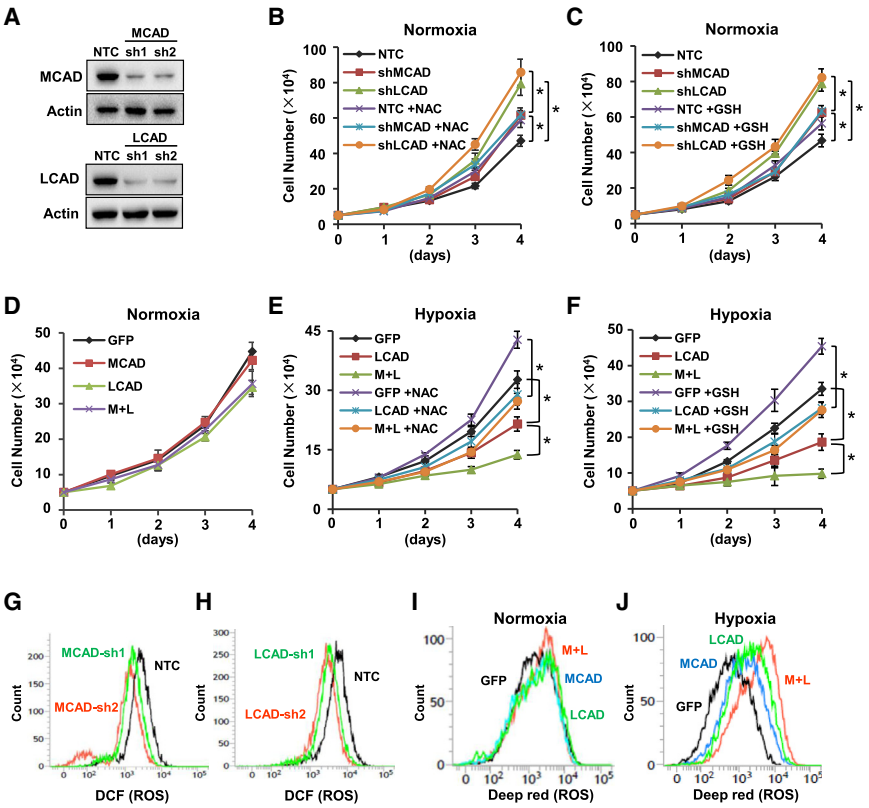

Figure 3. MCAD and LCAD Regulate Cell Proliferation in Part by Altering ROS in Cancer Cells

(A) Western blot analysis of MCAD and LCAD in Hep3B cells stably expressing NTC, shMCAD, or shLCAD.

(B and C) Cell growth curves of Hep3B cells stably expressing NTC, shMCAD, or shLCAD in the absence or presence of 5 mM NAC (B) or GSH (C) were determined by trypan blue counting.

(D) Cell growth curves of Hep3B cells stably expressing GFP, MCAD, LCAD, or M+L under normoxia were determined by trypan blue counting.

(E and F) Cell growth curves of Hep3B cells stably expressing GFP, LCAD, or M+L under hypoxia with or without 5 mM NAC (E) or GSH (F) were determined by trypan blue counting.

(G and H) ROS levels were measured by flow cytometry in Hep3B cells stably expressing NTC, shMCAD (G), or shLCAD (H) using the DCF fluorescence.

(I and J) ROS levels were measured by flow cytometry in Hep3B cells stably expressing GFP, MCAD, LCAD, or both (M+L) under normoxia (I) or hypoxia (J) using deep red fluorescence.

Data were presented as mean (±SD). *$p < 0.05$ as compared to corresponding control group. See also Figure S3.

cell proliferation in part by regulating ROS production. Cells overexpressing LCAD showed a significant growth disadvantage, even in the presence of NAC, suggesting that other mechanisms beyond ROS might be involved in the regulation of cell proliferation by LCAD.

To explore whether MCAD and LCAD regulate energy homeostasis, we measured ATP in Hep3B cells. Knockdown of MCAD or LCAD expression had no effect on cellular ATP levels under either normal or glutamine-free culture conditions (Figures S3H and S3I). However, ATP levels were significantly decreased in MCAD or LCAD knockdown Hep3B cells under glucose-free conditions (Figures S3H and S3I), suggesting that FAO could become a major source of ATP production in cancer cells in the absence of glucose. Consistent with this observation, when FAO was inhibited by etomoxir, or repressed by loss of function of MCAD and LCAD, glucose uptake and lactate production increased (Figures S3J and S3K), indicating that glycolytic metabolism in cancer cells is enhanced when FAO is inhibited. Conversely, accelerating FAO by co-overexpressing MCAD and LCAD attenuated hypoxia-induced glucose uptake and lactate production (Figures S3L and S3M), indicating that augmenting FAO inhibits glycolytic metabolism in cancer cells. Hypoxia induces increased glucose uptake and lactate production by upregulating expression of glycolytic genes, such as glucose transporter 1 (*GLUT1*) and lactate dehydrogenase A (*LDHA*). However, neither MCAD nor LCAD regulates expression of GLUT1 or LDHA (Figure S3N; data not shown). Instead, mRNA and protein expression of glucose transporter 2 (*GLUT2*) were significantly increased in Hep3B cells expressing shRNA targeting MCAD or LCAD (Figures S3N and S3O), suggesting that

(D) Hep3B cells were cultured under normoxia or hypoxia for 24 hr, followed by quantitative real-time PCR analyzing the mRNA expression of *PGC-1α*, *PGC-1β*, *PPRC1*, *PPARα*, *PPARδ* and *PPARγ*.

(E and F) mRNA (E) and protein (F) expression of PGC-1β, MCAD, and LCAD were measured in Hep3B cells stably expressing NTC or shRNAs targeting PGC-1β.

(G) Hep3B cells with stable expression of pMX empty vector (EV) or pMX-c-Myc were treated under normoxia or hypoxia for 48 hr, followed by protein analysis of PGC-1β, MCAD, and LCAD.

(H and I) Conversion of [1-^{14}C]-palmitic acid (H) or [1-^{14}C]-oleic acid (I) into ASM was measured in Hep3B cells stably expressing GFP, MCAD, LCAD, or both MCAD and LCAD cultured under normoxia or hypoxia for 48 hr.

(J) Protein expression of endogenous and exogenous MCAD and LCAD were analyzed in Hep3B cells stably expressing GFP, MCAD, LCAD, or both MCAD and LCAD cultured under normoxia or hypoxia for 48 hr.

(K and L) Conversion of [1-^{14}C]-palmitic acid (K) or [1-^{14}C]-oleic acid (L) into radioactive ASM or CO_2 was measured in Hep3B cells stably expressing NTC, LCAD shRNA (shLCAD), MCAD shRNA (shMCAD), or MCAD shRNA plus LCAD shRNA (shM+shL).

(M) Western blot analysis of MCAD and LCAD protein in Hep3B cells stably expressing NTC, shMCAD, shLCAD, or shM+shL.

β-actin serves as loading control in the western blot. Data were presented as mean (±SD). *$p < 0.05$ as compared to corresponding control group. See also Figure S2.

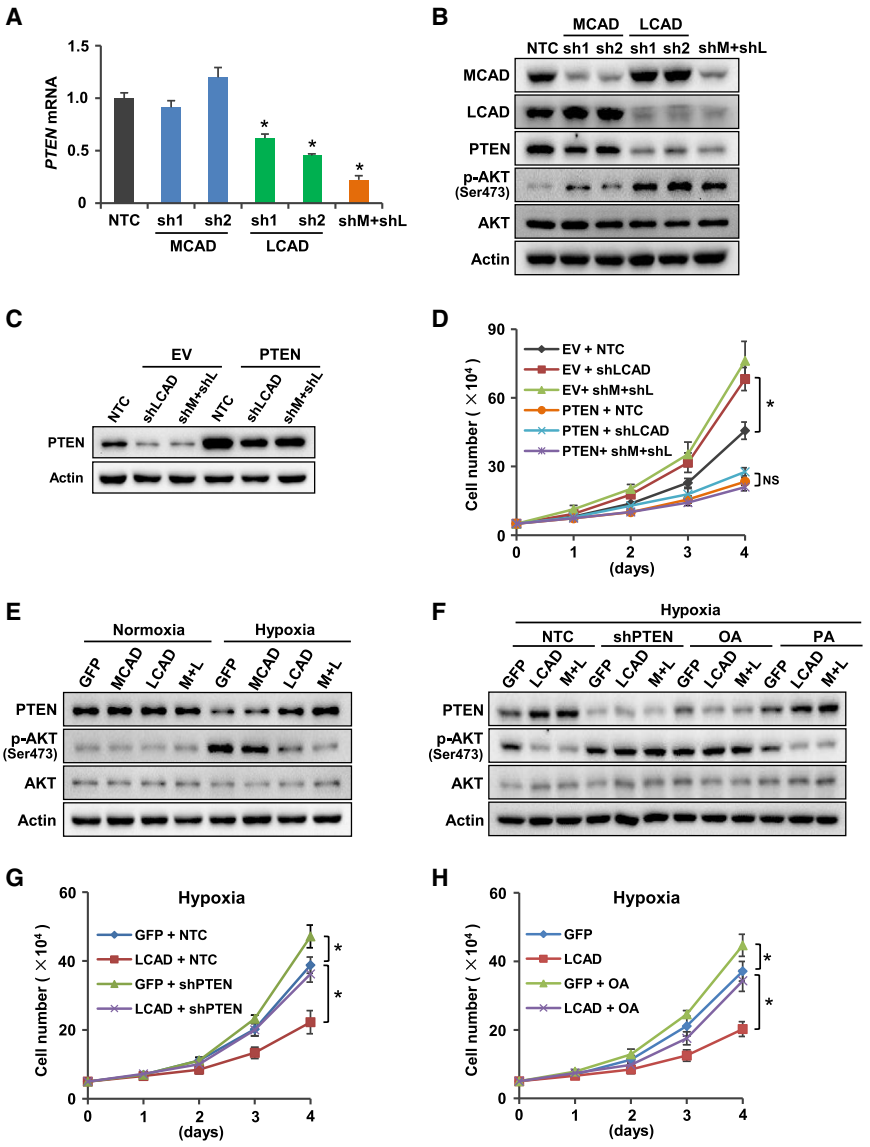

Figure 4. Depletion of LCAD Promotes Cancer Cell Proliferation by Reducing PTEN

(A and B) Quantitative real-time PCR analysis of *PTEN* mRNA expression (A) and western blot analysis of MCAD, LCAD, PTEN, serine 473 phosphorylation AKT (p-AKT), and AKT levels (B) were performed in Hep3B cells stably expressing NTC, shMCAD, shLCAD, or shM+shL.

(C and D) Hep3B cells stably expressing NTC, shLCAD, or shM+shL were further infected with viruses expressing pBABE EV or pBABE-PTEN. PTEN protein levels (C) and cell growth curve was determined (D).

(E) PTEN, p-AKT, and AKT levels were determined by western blot in Hep3B cells stably expressing GFP, MCAD, LCAD, or M+L under normoxia or hypoxia for 48 hr.

(F) Hep3B cells stably expressing GFP, MCAD, LCAD, or both MCAD and LCAD were further infected with viruses expressing NTC or PTEN shRNA (shPTEN) or cultured in the presence of 50 μM oleic acid (OA) or palmitic acid (PA). PTEN, p-AKT, and AKT levels were determined by western blot in those cells treated under hypoxic condition for 48 hr.

(G) Hep3B cells stably expressing GFP or LCAD were further infected with viruses expressing NTC or shPTEN, followed by cell growth curve analysis by trypan blue counting under hypoxic condition.

(H) Cell growth curves of Hep3B cells stably expressing GFP or LCAD in the presence or absence of 50 μM OA under hypoxic condition were determined by trypan blue counting.

β-actin serves as loading control in the western blot. Data were presented as mean (±SD). *$p < 0.05$ as compared to corresponding control group; NS, not significant. See also Figure S4

MCAD and LCAD may affect glucose uptake and glycolytic metabolism by regulating GLUT2 expression. Nevertheless, although our data demonstrating regulation of GLUT2 by MCAD and LCAD might provide a feedback mechanism for enhanced glucose uptake for ATP production when FAO is suppressed, unfortunately, it could not explain the differential effect of MCAD versus LCAD on cancer cell proliferation.

Depletion of LCAD Promotes Progression of Cancer Cells by Reduction of PTEN

The differential effect between MCAD and LCAD on cancer cell proliferation led us to search further for other mechanisms beyond ROS and ATP. Our data indicated that MCAD primarily mediates oxidation of palmitic acid (C16:0) and stearic acid (C18:0) (Figures 2H, 2K, S2M, and S2O), whereas LCAD mediates oxidation of oleic acid (C18:1) and linoleic acid (C18:2) (Figures 2I, 2L, S2N, and S2P). It has been reported that unsaturated fatty acids, including oleic acid and linoleic acid, facilitate cell proliferation by inhibiting transcription of the *PTEN* tumor suppressor gene in HCC (Vinciguerra et al., 2009). Knockdown of LCAD, but not MCAD, significantly decreased PTEN mRNA and protein expression in Hep3B cells (Figures 4A and 4B). Phosphorylation of serine 473 (S473) on AKT was significantly enhanced by knockdown of LCAD, but only marginally increased by MCAD knockdown (Figure 4B), indicating that AKT was activated by PTEN repression in cells with LCAD loss of function. To further address if PTEN is involved in LCAD-regulated cancer cell proliferation, we overexpressed PTEN in LCAD knockdown cells, which have low levels of endogenous PTEN (Figure 4C). Forced expression of PTEN diminished the growth advantage of LCAD knockdown cells (Figure 4D), demonstrating that PTEN repression is required for increased proliferation in cells with loss of LCAD expression.

Because hypoxic stress inhibits LCAD expression and induces accumulation of lipids (including both saturated and unsaturated fatty acids), we next analyzed PTEN expression and AKT activation under hypoxic stress. The results showed that hypoxia leads to suppression of PTEN expression and activation of AKT S473

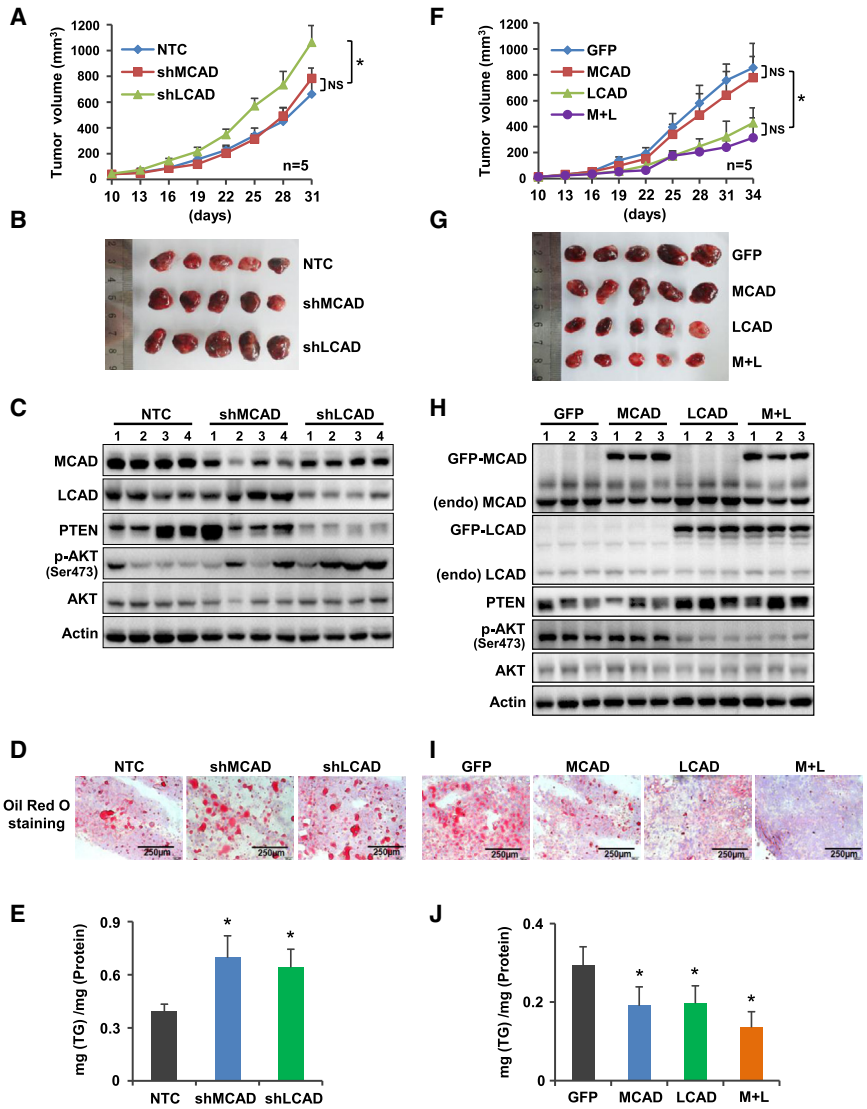

Figure 5. LCAD Suppresses Tumor Growth in Vivo

(A and B) Hep3B cells stably expressing NTC, shMCAD, or shLCAD were injected subcutaneously into nude mice (n = 5 for each group). Tumor growth curves were measured starting from 10 days after inoculation (A), and tumors were extracted and compared at the end of the experiment (B).

(C) Protein levels of MCAD, LCAD, PTEN, p-AKT, and AKT were determined by western blot using the lysates from four independent tumors of each group as in (B).

(D) Representative imaging of oil red O staining using the frozen sections of extracted tumors from different groups as in (B) was shown.

(E) TG concentrations in the lysates from extracted tumors in (B) were measured by triglyceride detection kit, and the values were normalized to protein.

(F and G) Hep3B cells stably expressing GFP, MCAD, LCAD, or M+L were injected subcutaneously into nude mice (n = 5 for each group). Tumor growth curves were measured starting from 10 days after inoculation (F), and tumors were extracted and compared at the end of the experiment (G).

(H) Protein levels of endogenous and exogenous MCAD and LCAD, PTEN, p-AKT, and AKT were determined by western blot using the lysates from three independent tumors of each group as in (G).

(I) Representative imaging of oil red O staining using the frozen sections of extracted tumors from different groups as in (G) was shown.

(J) TG concentrations in the lysates from extracted tumors in (G) were measured by triglyceride detection kit, and the values were normalized to protein.

β-actin serves as loading control in the western blot. Data were presented as mean (±SD). *$p < 0.05$ as compared to corresponding control group; NS, not significant. See also Figure S5.

phosphorylation, which were reversed by forced expression of LCAD (Figure 4E). To further confirm that the PTEN pathway is involved in LCAD-induced inhibition of cell proliferation, we knocked down PTEN in LCAD-overexpressing Hep3B cells (Figure 4F). Western blot results demonstrated that downregulation of PTEN counteracted the inhibitory effect of LCAD on AKT phosphorylation under hypoxic conditions (Figure 4F). More importantly, knocking down PTEN diminished the inhibitory effect of LCAD on cell proliferation under hypoxic stress (Figure 4G), further demonstrating that PTEN is required for the regulation of cell proliferation by LCAD. Addition of oleic acid, but not palmitic acid, into cell-culture media inhibited PTEN expression and enhanced S473 phosphorylation of AKT in hypoxic Hep3B cells (Figure 4F). Addition of oleic acid also counteracted the inhibitory effect of LCAD on cell proliferation (Figure 4H), suggesting that decreased oleic acid levels are responsible for cell growth inhibition in cells with LCAD overexpression. Because oleic acid and palmitic acid differ both with respect to saturation and carbon chain length, we designed experiments to determine whether saturation or chain length of fatty acids affects PTEN expression and cell growth. Both western blot and cell growth curves showed that only unsaturated fatty acids such as oleic acid (C18:1) and palmitoleic acid (C16:1), but not saturated stearic acid (C18:0) or palmitic acid (16:0), inhibited PTEN expression and stimulated cell growth in Hep3B cells (Figures S4A and S4B). Taken together, our results indicate that, besides ROS, LCAD, but not MCAD, also inhibits cell proliferation under hypoxia via enhanced PTEN expression.

LCAD Suppresses Tumor Growth In Vivo

Analysis of mouse xenografts using Hep3B cells that stably expressed shRNA targeting LCAD or MCAD showed that knockdown of LCAD, but not MCAD, significantly enhanced tumor volume (Figures 5A and 5B) and mass (Figure S5A) as compared to the nontargeting control group. Consistent with the in vitro data, lysates from tumor tissues revealed that tumors generated

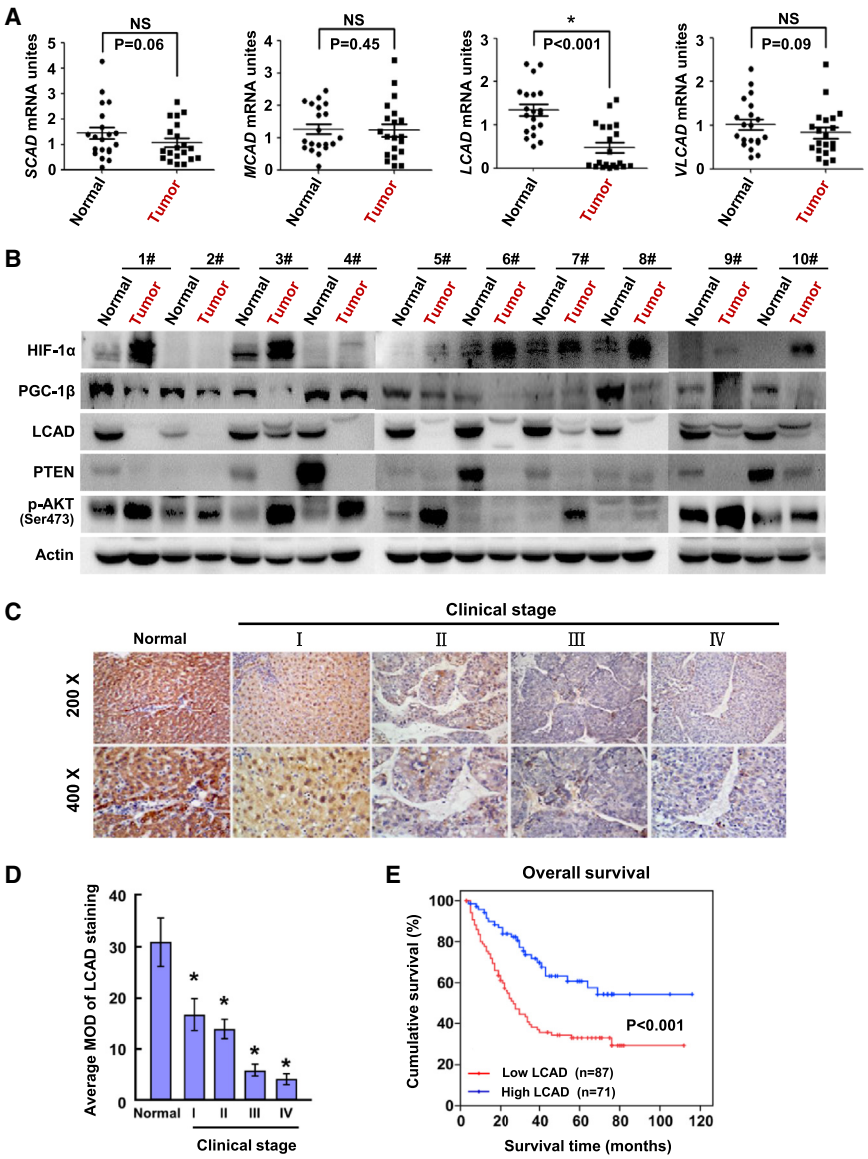

Figure 6. LCAD Deficiency Correlates with Human HCC and Predicts Poor Clinical Prognosis

(A) mRNA expressions of *SCAD*, *MCAD*, *LCAD*, and *VLCAD* were determined by quantitative real-time PCR in 20 pairs of clinically matched tumor adjacent noncancerous liver tissues (normal) and human HCC tissues (tumor). mRNA levels were normalized to 18S.

(B) HIF-1α, PGC-1β, LCAD, PTEN, and p-AKT were determined by western blot using the paired tumor adjacent noncancerous liver tissues and human HCC tissues.

(C) Representative IHC analysis of LCAD expression in normal liver tissues (normal) and HCC specimens of different clinical stages (I–IV) was shown.

(D) Statistical quantification of the mean optical density (MOD) values of LCAD staining in IHC assay between normal liver tissues and HCC specimens of different clinical stages (I–IV). The MOD of LCAD staining decreases as HCC progresses to a higher clinical stage.

(E) Kaplan-Meier curves with univariate analyses for patients with low versus high LCAD expression. β-actin serves as loading control in the western blot. Data were presented as mean (±SD). *p < 0.05 as compared to corresponding control group; NS, not significant. See also Tables S1–S4.

from LCAD knockdown cells, but not those of MCAD knockdown cells, had lower PTEN expression and elevated phosphorylation of AKT at S473 (Figure 5C). On the other hand, forced expression of LCAD, but not MCAD, markedly reduced tumor volume (Figures 5F and 5G) and mass (Figure S5B), indicating that LCAD, but not MCAD, is critical for regulation of tumor growth. Enhanced PTEN expression and reduced AKT phosphorylation were observed in tumors generated from LCAD-overexpressing cells (Figure 5H). Oil red O staining of frozen sections and TG content measurement in tissue lysates revealed that downregulation of MCAD- or LCAD-stimulated lipid accumulation (Figures 5D and 5E), whereas overexpression of MCAD or LCAD decreased lipid storage compared to the control group (Figures 5I and 5J), which are consistent with data from in vitro experiments. Also, these data are consistent with previously reports that MCAD- or LCAD-deficient mice have abnormal lipid accumulation in the liver (Kurtz et al., 1998; Tolwani et al., 2005).

Decreased LCAD Expression in HCC Predicts Patient Mortality

Analysis of cell proliferation in vitro and tumor growth in vivo indicated that LCAD has a tumor-suppressive effect. To investigate the physiological significance of this regulatory pathway, LCAD expression was also studied in 20 paired HCC lesions and adjacent noncancerous tissue samples. Among the acyl-CoA dehydrogenases, only *LCAD* mRNA levels were significantly decreased in HCC lesions as compared to adjacent normal tissue (Figure 6A). Although *MCAD* expression is decreased by hypoxic stress in cultured cells, we did not observe any significant difference in mRNA expression between HCC lesions and adjacent normal tissue (Figure 6A). Further, western blot assays showed decreased PGC-1β, LCAD, PTEN protein levels and enhanced HIF-1α and AKT phosphorylation levels in HCC tissue as compared to adjacent normal tissue (Figure 6B).

Next, immunohistochemistry (IHC) was employed to analyze LCAD expression in a retrospective cohort of 158 clinicopathologically characterized HCC cases, including ten cases of stage I (6.3%), 106 cases of stage II (67.1%), 33 cases of stage III (20.9%), and nine cases of stage IV (5.7%) liver cancer, based on the TNM staging (Table S1). IHC results revealed that LCAD protein was abundantly expressed in normal liver, weakly expressed in early-stage HCC (TNM stages I and II) and barely detectable in late-stage HCC (TNM stages III and IV) (Figure 6C). Image analysis of the IHC revealed that LCAD expression in

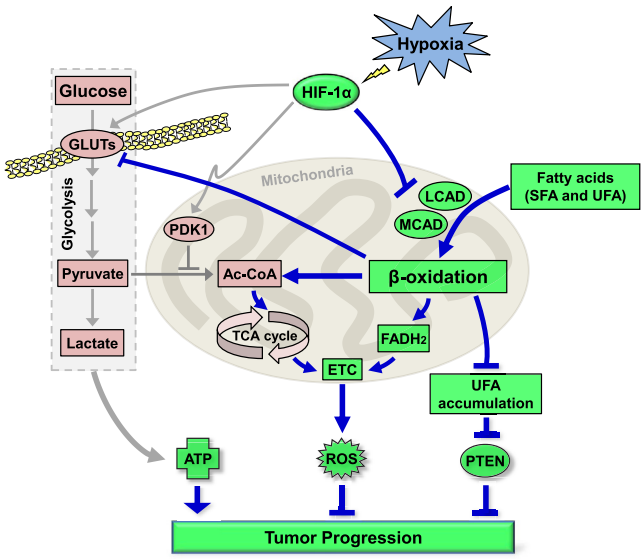

Figure 7. HIF-1-Mediated Suppression of Fatty Acid Oxidation Is Critical for Cancer Progression

HIF-1 has been well defined to facilitate glycolysis under hypoxic stress in cancer cells. Here, we depict that HIF-1α inhibits β-oxidation by repressing the expression of MCAD and LCAD (in green), two family members of acyl-CoA dehydrogenases that catalyze the first step of β-oxidation in mitochondria. Both MCAD- and LCAD-regulated fatty acid oxidation facilitates tumor cell proliferation by altering ROS levels and glycolysis. However, deficiency of LCAD-induced unsaturated fatty acid oxidation possesses the most potent effect on cancer progression by regulating the PTEN pathway. See text for details.

clinical stage I–IV primary tumors was significantly decreased compared to normal liver (Figure 6D). Furthermore, LCAD was drastically downregulated in late-stage HCC (stages III and IV) as compared to early-stage HCC (stages I and II) (Figure 6D; Table S2), suggesting that LCAD expression was gradually decreased as HCC progressed to a higher clinical stage. Further, Spearman analysis revealed correlations between LCAD expression and patient clinicopathological characteristics, including survival time, vital status, clinical stage, and tumor size (Table S3), further suggesting a strong association of LCAD expression with HCC clinical staging and patient survival. Univariate analysis revealed that, together with TNM stage and tumor size, LCAD level is a significant prognostic factor. Multivariate analysis also demonstrated that LCAD expression and clinical TNM staging are predictive of the overall survival of HCC patients (Table S4). Finally, Kaplan-Meier test indicated that LCAD expression in HCC patients was significantly associated with survival time, with patients expressing high LCAD in their HCC lesions surviving much longer than those with low LCAD expression (Figure 6E), suggesting that LCAD protein may represent a promising prognostic biomarker in HCC.

DISCUSSION

There is a growing appreciation that cancer cells generally undergo comprehensive metabolic reprogramming, which generally permits rapid growth and allow adaptation to the tumor microenvironment (DeBerardinis et al., 2008). HIFs have been intensively investigated for their roles in metabolic reprogramming (Semenza, 2010). Nevertheless, whereas hypoxia- and HIF-dependent regulation of glycolysis, glutaminolysis, and lipid synthesis have been demonstrated (Kim et al., 2006; Furuta et al., 2008; Metallo et al., 2012), the effect of hypoxia and HIFs on FAO in cancer cells had not been clearly elucidated. In this regard, it is significant that we establish here a previously unappreciated mechanism by which HIF-1 suppresses acyl-CoA dehydrogenases and FAO in hypoxic cells to facilitate cancer progression. It is intriguing to note that, whereas we observed similar roles for both HIF-1 and HIF-2 in causing lipid accumulation in hypoxic cancer cells (Figures 1D and 1E), only HIF-1 suppresses expression of acyl-CoA dehydrogenases and FAO (Figures 1I, 1J, and 2C), highlighting overlapping but differential roles for HIF-1 and HIF-2 in regulating lipid metabolism of cancer cells.

It has been documented recently that lipid synthesis is regulated by hypoxia stress in cancer cells (Anastasiou and Cantley, 2012). We also observed the enhanced expression of genes for FAS in HCC cells (Figure 1F). Proliferating cancer cells require lipid for cellular membrane synthesis and other essential functions. Cancer cells generally adopt a de novo lipid synthesis strategy rather than use of stored lipids, and, as a result, accumulation of lipid droplets is commonly observed in cancer cells (Kuhajda, 2000). Hence, one would expect reduced lipid catabolism in cancer cells to sustain rapid cell proliferation. Nevertheless, recent results from several groups did not seem to be in agreement with this expectation. In contrast, prosurvival roles have been reported for FAO under various conditions (Deberardinis et al., 2006; Zaugg et al., 2011). It is interesting that we demonstrate that, whereas enhanced FAO under normoxic conditions does not affect cancer cell growth, it is detrimental under hypoxia. Hence, we assume that previous observations of FAO as beneficial for cancer proliferation may be context dependent or cancer cell type specific, as demonstrated by different consequences of FAO alteration reported by different groups (Deberardinis et al., 2006; Zaugg et al., 2011). Importantly, at least in the multiple cancer cell lines studied here, we provide clear evidence showing that HIF-1α-mediated suppression of FAO is beneficial for cancer proliferation via reduced ROS production, enhanced Glut2 expression and glycolysis, and activation of prosurvival cancer signaling (Figure 7).

It was surprising that the expression of LCAD but not MCAD was suppressive to cancer growth. LCAD and MCAD both catabolize the first step of FAO in mitochondria but differ, according to the original definitions, in the chain length of their fatty acid substrates. Nevertheless, LCAD is also known to mediate unsaturated fatty acid oxidation, whereas MCAD prefers saturated fatty acids as substrates. As a result, only loss of LCAD, but not MCAD, will lead to accumulation of unsaturated fatty acids. Kidwell et al. reported the requirements of unsaturated fatty acids for growth and survival of a rat mammary tumor cell line (Kidwell et al., 1978). Animals fed a diet high in unsaturated fatty acids were found to be more susceptible to cancer development (Bartsch et al., 1999). Unsaturated fatty acids inhibit PTEN via miR-21 upregulation in hepatocytes (Vinciguerra et al., 2009). This led us to hypothesize that loss of LCAD, but not MCAD, led to accumulation of unsaturated fatty acids, which, in turn,

suppress PTEN, resulting in cancer progression. Indeed, our results confirmed that only the unsaturated fatty acids oleic acid and palmitoleic acid blunted PTEN expression in cultured cells (Figure S4A). Importantly, our in vivo results from mouse tumor xenograft models demonstrated that loss of LCAD, but not MCAD, resulted in suppression of PTEN in vivo and enhanced tumor growth (Figures 5A–5C). Our discovery establishes a mechanism by which reprogrammed lipid metabolism in cancer cells promotes proliferation by crosstalk with signal transduction pathways.

Accumulating clinical evidence suggests that lipid disorders are correlated with cancer incidence. Calle et al. reported that up to 20% of all deaths from cancer are related to obesity (Calle et al., 2003). In fact, alterations of many metabolism-related genes, such as *IDH1*, *IDH2*, *FH*, *SDH*, and *PKM2*, have been identified to cause human malignancies (Thompson, 2009). Hence, it is very interesting to observe that decreased expression of LCAD led to suppression of PTEN, whose deletion or diminished expression in HCC was associated with a poor prognosis (Vinciguerra and Foti, 2008), suggesting a suppressive role for LCAD in human malignancies. Among the family members of acyl-CoA dehydrogenase, whereas SCAD, MCAD, and VLCAD are implicated in human inherited disorders of fatty acid oxidation (Lea et al., 2000), there is no similar report involving LCAD in any human diseases, at least to the best of our knowledge. Of note, a thorough search and analysis of publicly available data sets led us to the discovery of one oncomine data set (Data Link: http://www.ncbi.nlm.nih.gov/geo/query/acc.cgi?acc=GSE14520), in which the expression of LCAD was comprehensively suppressed in human liver cancers (Roessler et al., 2010). However, those alterations had never been specifically studied. In this regard, it is very interesting that, besides results from cancer cell lines and mouse tumor models to demonstrate the role of HIF-1-mediated suppression of LCAD in cancer progression, we identified in 158 clinical HCC samples that loss of LCAD is correlated with poor clinical prognosis of HCC. Hence, our discovery in this study is highly relevant to human cancers. Although further endeavors are under way to determine whether alterations in LCAD expression and activity in hepatocytes are reliable prognostic markers for HCC, it is safe to predict that understanding the molecular mechanisms regulating lipid metabolism in cancer cells and their connection to activated signal transduction pathways that promote cancer cell proliferation and survival will provide opportunities to design novel therapeutic strategies to harness human malignancies.

EXPERIMENTAL PROCEDURES

Cell Culture and Reagents

Human 293T, Hep3B, HepG2, SK-Hep-1, MCF-7, and RCC4 cells were cultured in Dulbecco's modified essential medium (DMEM). PC3 and P493 cells were cultured in RPMI-1640. The media were supplemented with 10% FBS and 1% penicillin-streptomycin. Mouse embryo fibroblasts (MEFs) were cultured in DMEM with 15% FBS, 2 mM sodium pyruvate, nonessential amino acids, and 1% penicillin-streptomycin.

Plasmids and Establishing Stable Cells

shRNAs targeting HIF-1α or HIF-2α were inserted into pRPL-GFP-Puro vector as previously reported (Zhang et al., 2012). shRNAs targeting MCAD, LCAD, c-Myc, PGC-1β, or PTEN were purchased from Sigma-Aldrich. Expression vector pMX-c-Myc was purchased from Addgene (Plasmid 17220). CDS sequence of human *MCAD* or *LCAD* was inserted into pSIN-GFP lentiviral vector at BamHI and SpelSites. CDS sequence of human *PTEN* was inserted into pBABE lentiviral vector at BamHI and EcoRI sites. Transduction and viral infection was performed as previously described (Zhang et al., 2007).

Nile Red Staining and Triglyceride Measurement

To visualize lipid droplets, cultured cells were fixed with 4% paraformaldehyde and then stained with 0.05 μg/ml Nile red (19123; Sigma-Aldrich) for 10 min followed by PBS washing and DAPI staining. Imagings were visualized by immunofluorescence microscopy. For triglyceride measurement, cells were collected and lysed with RIPA buffer supplied with 1% NP-40 for 30 min, equal volume of cell lysates were used to measure triglyceride using a Biochemical Triglyceride Determination Kit (F001-2; NJJC Bio). The triglyceride values were normalized to cellular protein measured with Bradford Protein Assay Kit (SK3031; Sangon Bio).

Fatty Acid β-Oxidation

For measurement of palmitic acid, stearic acid, oleic acid, or linoleic acid oxidation, cells were incubated at 37°C in DMEM supplied with 1 μCi/ml [1-^{14}C]-palmitic acid, [1-^{14}C]-stearic acid, [1-^{14}C]-oleic acid, or [1-^{14}C]-linoleic acid (PerkinElmer Life and Analytical Sciences), 1 mM nonradioactive palmitic acid, stearic acid, oleic acid, or linoleic acid, 10 mM HEPES, and 0.5% fatty acid free BSA (Sigma-Aldrich), as previous reported (Kim et al., 2000). Produced $^{14}CO_2$ on the filter paper and ^{14}C-ASM in the supernatant were determined by scintillation counting (PerkinElmer; Tri-Carb). Values were normalized to protein quantification of cell lysate.

Western Blot

Cells were lysated with RIPA buffer and equal amounts of protein in the lysates were boiled and fractionated by 7%–10% SDS-PAGE. Primary antibodies against the following proteins were used: HIF-1α (BD Bioscience); HIF-2α, c-Myc, and PGC-1β (Santa Cruz Biotechnology); β-actin, α-tubulin (Abmart); SCAD, MCAD, LCAD, VLCAD, ACSL1, CPT1A, CPT1C, GLUT1, and GLUT3 (Proteintech); GLUT2 (Millipore); PTEN (Cascade); VDAC, AKT, and p-AKT (ser 473) (CST). Horseradish-peroxidase-conjugated anti-rabbit and anti-mouse (Bio-Rad) secondary antibodies were used. Signal was detected using Western ECL Substrate (Bio-Rad).

Quantitative Real-Time PCR

Primer sequences were showed in Table S5, quantitative real-time PCR was performed using iScript SYBR Green PCR Kit (Bio-Rad) on a Bio-Rad iCycler.

Animal Studies

All animal studies were conducted with approval from the Animal Research Ethics Committee of the University of Science and Technology of China. For xenograft experiments, different Hep3B cell lines were injected subcutaneously into nude mice (SJA Laboratory Animal Company). Ten days after injection, tumor volumes were measured every 3 days with a caliper and calculated using the equation, volume = width * depth * length * 0.52.

Oil Red O Staining

Frozen sections from mice subcutaneous tumors were fixed in 10% formalin, washed with 60% propylene glycerol, and then stained with 0.5% oil red O (Sangon Bio) in propylene glycerol for 10 min at 60°C. The red lipid droplets were visualized by microscopy.

Clinical Human Tissue Specimen

The normal liver tissues were collected from patients undergoing resection of hepatic hemangiomas at the Department of Hepatobiliary Surgery, the First Affiliated Hospital of Sun Yat-sen University. Formalin-fixed, paraffin-embedded primary HCC specimens obtained from 158 patients were randomly selected from the archives of the Sun Yat-sen University Cancer Center (Guangzhou, China). The 20 paired HCC lesions and the adjacent noncancerous clinical tissue samples were collected from HCC patients. For use of these clinical materials for research purposes, prior patients' written

informed consents and approval from the Institutional Research Ethics Committee of Sun Yat-sen University Cancer Center were obtained. Tumor clinical stages were defined according to the 2002 American Joint Committee on Cancer/International Union against Cancer tumor/lymph node metastasis/distal metastasis (TNM) classification system.

Statistical Analysis

The relationship between LCAD expression and clinicopathological characteristics was analyzed by the chi-square test. Survival curves were plotted by the Kaplan-Meier method and compared using the log-rank test. Data are presented as the mean (±SD) of at least three independent experiments. Statistical significance ($p < 0.05$) was assessed by the Student's t test unless otherwise noted.

SUPPLEMENTAL INFORMATION

Supplemental Information includes Supplemental Experimental Procedures, five figures, and five tables and can be found with this article online at http://dx.doi.org/10.1016/j.celrep.2014.08.028.

ACKNOWLEDGMENTS

Our work is supported in part by National Basic Key Research Program of China (2014CB910601, 2014CB910604, and 2012CB910104), Chinese Academy of Sciences (XDA01010404), National Nature Science Foundation of China (31171358, 31371429, 81372148, and 31071257). H.Z. is supported by Chinese Government "1000 Youth Talent Program."

Received: April 29, 2014
Revised: July 16, 2014
Accepted: August 13, 2014
Published: September 18, 2014

REFERENCES

Anastasiou, D., and Cantley, L.C. (2012). Breathless cancer cells get fat on glutamine. Cell Res. *22*, 443–446.

Bartsch, H., Nair, J., and Owen, R.W. (1999). Dietary polyunsaturated fatty acids and cancers of the breast and colorectum: emerging evidence for their role as risk modifiers. Carcinogenesis *20*, 2209–2218.

Calle, E.E., Rodriguez, C., Walker-Thurmond, K., and Thun, M.J. (2003). Overweight, obesity, and mortality from cancer in a prospectively studied cohort of U.S. adults. N. Engl. J. Med. *348*, 1625–1638.

DeBerardinis, R.J., and Thompson, C.B. (2012). Cellular metabolism and disease: what do metabolic outliers teach us? Cell *148*, 1132–1144.

Deberardinis, R.J., Lum, J.J., and Thompson, C.B. (2006). Phosphatidylinositol 3-kinase-dependent modulation of carnitine palmitoyltransferase 1A expression regulates lipid metabolism during hematopoietic cell growth. J. Biol. Chem. *281*, 37372–37380.

DeBerardinis, R.J., Lum, J.J., Hatzivassiliou, G., and Thompson, C.B. (2008). The biology of cancer: metabolic reprogramming fuels cell growth and proliferation. Cell Metab. *7*, 11–20.

Espinoza, D.O., Boros, L.G., Crunkhorn, S., Gami, H., and Patti, M.E. (2010). Dual modulation of both lipid oxidation and synthesis by peroxisome proliferator-activated receptor-gamma coactivator-1alpha and -1beta in cultured myotubes. FASEB J. *24*, 1003–1014.

Furuta, E., Pai, S.K., Zhan, R., Bandyopadhyay, S., Watabe, M., Mo, Y.Y., Hirota, S., Hosobe, S., Tsukada, T., Miura, K., et al. (2008). Fatty acid synthase gene is up-regulated by hypoxia via activation of Akt and sterol regulatory element binding protein-1. Cancer Res. *68*, 1003–1011.

Hanahan, D., and Weinberg, R.A. (2011). Hallmarks of cancer: the next generation. Cell *144*, 646–674.

Huss, J.M., Levy, F.H., and Kelly, D.P. (2001). Hypoxia inhibits the peroxisome proliferator-activated receptor alpha/retinoid X receptor gene regulatory pathway in cardiac myocytes: a mechanism for O2-dependent modulation of mitochondrial fatty acid oxidation. J. Biol. Chem. *276*, 27605–27612.

Kidwell, W.R., Monaco, M.E., Wicha, M.S., and Smith, G.S. (1978). Unsaturated fatty acid requirements for growth and survival of a rat mammary tumor cell line. Cancer Res. *38*, 4091–4100.

Kim, J.Y., Hickner, R.C., Cortright, R.L., Dohm, G.L., and Houmard, J.A. (2000). Lipid oxidation is reduced in obese human skeletal muscle. Am. J. Physiol. Endocrinol. Metab. *279*, E1039–E1044.

Kim, J.W., Tchernyshyov, I., Semenza, G.L., and Dang, C.V. (2006). HIF-1-mediated expression of pyruvate dehydrogenase kinase: a metabolic switch required for cellular adaptation to hypoxia. Cell Metab. *3*, 177–185.

Krishnan, J., Suter, M., Windak, R., Krebs, T., Felley, A., Montessuit, C., Tokarska-Schlattner, M., Aasum, E., Bogdanova, A., Perriard, E., et al. (2009). Activation of a HIF1alpha-PPARgamma axis underlies the integration of glycolytic and lipid anabolic pathways in pathologic cardiac hypertrophy. Cell Metab. *9*, 512–524.

Kuhajda, F.P. (2000). Fatty-acid synthase and human cancer: new perspectives on its role in tumor biology. Nutrition *16*, 202–208.

Kunau, W.H., Dommes, V., and Schulz, H. (1995). beta-oxidation of fatty acids in mitochondria, peroxisomes, and bacteria: a century of continued progress. Prog. Lipid Res. *34*, 267–342.

Kurtz, D.M., Rinaldo, P., Rhead, W.J., Tian, L., Millington, D.S., Vockley, J., Hamm, D.A., Brix, A.E., Lindsey, J.R., Pinkert, C.A., et al. (1998). Targeted disruption of mouse long-chain acyl-CoA dehydrogenase gene reveals crucial roles for fatty acid oxidation. Proc. Natl. Acad. Sci. USA *95*, 15592–15597.

Lea, W., Abbas, A.S., Sprecher, H., Vockley, J., and Schulz, H. (2000). Long-chain acyl-CoA dehydrogenase is a key enzyme in the mitochondrial beta-oxidation of unsaturated fatty acids. Biochim. Biophys. Acta *1485*, 121–128.

Lin, J., Yang, R., Tarr, P.T., Wu, P.H., Handschin, C., Li, S., Yang, W., Pei, L., Uldry, M., Tontonoz, P., et al. (2005). Hyperlipidemic effects of dietary saturated fats mediated through PGC-1beta coactivation of SREBP. Cell *120*, 261–273.

Menendez, J.A., and Lupu, R. (2007). Fatty acid synthase and the lipogenic phenotype in cancer pathogenesis. Nat. Rev. Cancer *7*, 763–777.

Metallo, C.M., Gameiro, P.A., Bell, E.L., Mattaini, K.R., Yang, J., Hiller, K., Jewell, C.M., Johnson, Z.R., Irvine, D.J., Guarente, L., et al. (2012). Reductive glutamine metabolism by IDH1 mediates lipogenesis under hypoxia. Nature *481*, 380–384.

Mylonis, I., Sembongi, H., Befani, C., Liakos, P., Siniossoglou, S., and Simos, G. (2012). Hypoxia causes triglyceride accumulation by HIF-1-mediated stimulation of lipin 1 expression. J. Cell Sci. *125*, 3485–3493.

Roessler, S., Jia, H.L., Budhu, A., Forgues, M., Ye, Q.H., Lee, J.S., Thorgeirsson, S.S., Sun, Z., Tang, Z.Y., Qin, L.X., and Wang, X.W. (2010). A unique metastasis gene signature enables prediction of tumor relapse in early-stage hepatocellular carcinoma patients. Cancer Res. *70*, 10202–10212.

Semenza, G.L. (2010). HIF-1: upstream and downstream of cancer metabolism. Curr. Opin. Genet. Dev. *20*, 51–56.

Thompson, C.B. (2009). Metabolic enzymes as oncogenes or tumor suppressors. N. Engl. J. Med. *360*, 813–815.

Tolwani, R.J., Hamm, D.A., Tian, L., Sharer, J.D., Vockley, J., Rinaldo, P., Matern, D., Schoeb, T.R., and Wood, P.A. (2005). Medium-chain acyl-CoA dehydrogenase deficiency in gene-targeted mice. PLoS Genet. *1*, e23.

Vander Heiden, M.G.V., Cantley, L.C., and Thompson, C.B. (2009). Understanding the Warburg effect: the metabolic requirements of cell proliferation. Science *324*, 1029–1033.

Vinciguerra, M., and Foti, M. (2008). PTEN at the crossroad of metabolic diseases and cancer in the liver. Ann. Hepatol. *7*, 192–199.

Vinciguerra, M., Sgroi, A., Veyrat-Durebex, C., Rubbia-Brandt, L., Buhler, L.H., and Foti, M. (2009). Unsaturated fatty acids inhibit the expression of tumor suppressor phosphatase and tensin homolog (PTEN) via microRNA-21 up-regulation in hepatocytes. Hepatology *49*, 1176–1184.

Zaugg, K., Yao, Y., Reilly, P.T., Kannan, K., Kiarash, R., Mason, J., Huang, P., Sawyer, S.K., Fuerth, B., Faubert, B., et al. (2011). Carnitine palmitoyltransferase 1C promotes cell survival and tumor growth under conditions of metabolic stress. Genes Dev. *25*, 1041–1051.

Zhang, H., Gao, P., Fukuda, R., Kumar, G., Krishnamachary, B., Zeller, K.I., Dang, C.V., and Semenza, G.L. (2007). HIF-1 inhibits mitochondrial biogenesis and cellular respiration in VHL-deficient renal cell carcinoma by repression of C-MYC activity. Cancer Cell *11*, 407–420.

Zhang, H., Wong, C.C., Wei, H., Gilkes, D.M., Korangath, P., Chaturvedi, P., Schito, L., Chen, J., Krishnamachary, B., Winnard, P.T., Jr., et al. (2012). HIF-1-dependent expression of angiopoietin-like 4 and L1CAM mediates vascular metastasis of hypoxic breast cancer cells to the lungs. Oncogene *31*, 1757–1770.